

# Disks in Expanding FRW Universes

A. Feinstein, J. Ibáñez and Ruth Lazkoz  
 Dpto. Física Teórica, Universidad del País Vasco,  
 Apdo. 644, E-48080 Bilbao, Spain;  
 wtpfexxa@lg.ehu.es, wtpibmej@lg.ehu.es and wtblasar@lg.ehu.es

## ABSTRACT

We construct exact solutions to Einstein equations which represent relativistic disks imbedded in an expanding FRW Universe. It is shown that the expansion influences the kinematical characteristics of the disks such as rotational curves, surface mass density, etc. The effects of the expansion are exemplified with non-static generalizations of Kuzmin-Curzon and Schwarzschild disks.

*Subject headings:* celestial mechanics, stellar dynamics — cosmology: large scale structure of the Universe — galaxies: kinematics and dynamics — ISM: kinematics and dynamics — relativity

## 1. Introduction

Recently, there has been a renewed interest in the study of relativistic disks (Bičák, Lynden-Bell & Katz, 1993; Bičák & Ledvinka, 1993; & Bičák, Lynden-Bell & Pichon, 1993), stemming from a desire to address the possible observational evidence of giant black holes sustained by the surrounding disks. The gravitational fields of galactic disks may be accurately modeled by the Newtonian potential theory provided the thickness of the disk is negligible compared with the typical size of their halos. In more sound situations, however, when gravity is strong enough one must turn to General Relativity. A typical situation, where it is believed that Einstein theory may contribute is met when one considers the accretion disks around the central black holes in quasars. Disks may be also used to model sheet-like structures, so their study may shed some light on the understanding of the large scale inhomogeneities present in the Universe (Lemos & Ventura 1994).

In General Relativity, solutions representing thin disks may be constructed starting with static axially symmetric vacuum Weyl metrics. A discontinuity is then introduced in the first derivative of the metric across the azimuthal plane  $z = 0$ , which in turn induces distribution-like terms in the Ricci tensor. Everywhere outside the  $z = 0$  plane the solution is vacuum with a non-vanishing surface mass density concentrated on this plane. Since Weyl solutions are static, they should represent static disks. To allow for rotation in General Relativity one must drop the assumption of the orthogonality of the two Killing vector fields associated with Weyl geometry, thus complicating the problem by introducing the dragging of inertial frames.

Fortunately, Morgan and Morgan (1969a; 1969b; 1970) had the very smart idea of interpreting the “static disks” as made out of two equal streams of collisionless particles circulating in opposite directions. Consequently, the total angular momentum vanishes and the system may be described by a Weyl line element. Interestingly enough, there exists observational evidence of some galaxies with two counterrotating stellar components around their center (Rix, Franx, Fisher & Illingworth 1992; Merrifield & Kuijken 1994; Bertola et al. 1996; Kuijken, Fisher & Merrifield 1996).

Another interpretational problem with the solutions described by the Weyl metric arises due to the fact that the disks are infinite in their extent. One may argue, however, that infinite disks model the inner portions of galaxies or accretion disks. Once the interpretational problems are dealt with, it is not difficult to model relativistic disks and study their physical properties such as velocity profiles, surface mass density, redshifts and so on.

Evans and de Zeeuw (1992) showed that it is possible to analyze any classical axially symmetric disk into a linear superposition of so-called Kuzmin disks (Kuzmin 1956). Using this result, Bičák, Lynden-Bell and Katz (1993, hereafter BLK) constructed families of counterrotating disk space-times. Their work was further extended by Bičák, Lynden-Bell and Pichon (1993, hereafter BLP) and more recently by Lynden-Bell and Pichon (1996). On the other hand, Lemos and Letelier (1993; 1994; 1996) using the well known techniques of superposing different Weyl solutions, have constructed space-times describing disks surrounding Schwarzschild black holes.

The main purpose of this paper is to consider, in the framework of exact solutions in General Relativity, the effect of the cosmological expansion on the disk dynamics on one hand, and the influence of disk-like large-scale structures on the cosmological model's kinematics on the other. It is known (Noerdlinger & Petrosian 1971) that the effects of the expansion on bounded gravitational systems is proportional to the ratio  $\bar{\rho}/\rho_s$ , where  $\bar{\rho}$  is the background energy density and  $\rho_s$  is the mean rest-density of the system. Therefore, for galactic and accretion disks fueling the quasars these effects are not expected to be too significant, though the overall expansion may change the disk dynamics. For disk-like large-scale structures, however, the expansion may turn out to be of particular importance.

In §2 we propose an algorithm to generate solutions to Einstein equations which may be interpreted as inhomogeneities imbedded in a spatially flat isotropic Universe. The technique uses a scalar field generalization in a cosmological setting of static Weyl solutions. The scalar field can be split into two parts, one homogenous, which may be hydrodynamically interpreted as the velocity potential for an adiabatic perfect fluid acting as the source of a FRW expansion; and another one highly irregular which may be thought of as a local disk inhomogeneity. In §3 we apply the generating procedure of the previous section to the general relativistic Kuzmin disks. We then analyze the energy-momentum tensor for the obtained solutions and interpret them as disks imbedded in a FRW background. §4 is devoted to study the dynamics of the disks with the emphasis on the effects of the expansion on pertinent dynamical and kinematical quantities. We conclude the paper with the discussion and future prospects.

## 2. Exact non-static solutions with axial symmetry

### 2.1. The generating algorithm

In this Section we obtain non-static solutions to Einstein field equations representing compact objects in a cosmological setting. We start with Weyl's line element which can be written as:

$$ds^2 = -e^{2\nu(\rho,z)} dt^2 + e^{-2\nu(\rho,z)} \rho^2 d\phi^2 + e^{-2\nu(\rho,z)+2\zeta(\rho,z)} (d\rho^2 + dz^2). \quad (1)$$

Throughout the paper we use  $G = c = 1$ . It is well-known that vacuum static axially symmetric fields in General Relativity can be generated starting with a Newtonian potential (Weyl 1917; Levi-Civita 1919a; Levi-Civita 1919b). For the space-times obtained in this way the metric function  $\nu$  in equation (1) may be taken to be any classical solution of the Laplace equation in cylindrical coordinates, and the other metric function  $\zeta$  is obtained by a quadrature.

New non-static metrics may be generated in two stages. First, starting from a vacuum solution of the Einstein equations for a metric given by equation (1), we construct a new static solution with a minimally coupled massless scalar field  $\psi$  as a source. For these space-times the energy-momentum tensor takes the form:

$$T_{ab} = \psi_{,a}\psi_{,b} - \frac{1}{2}g_{ab}\psi_{,c}\psi^{,c}, \quad (2)$$

and the set of Einstein equations is

$$\nu_{zz} + \nu_{\rho\rho} + \rho^{-1}\nu_{\rho} = 0, \quad (3)$$

$$\zeta_{zz} + \zeta_{\rho\rho} - \rho^{-1}\zeta_{\rho} + 2\nu_{\rho}^2 = -\psi_{\rho}^2, \quad (4)$$

$$\zeta_{zz} + \zeta_{\rho\rho} + \rho^{-1}\zeta_{\rho} + 2\nu_z^2 = -\psi_z^2, \quad (5)$$

$$\rho^{-1}\zeta_z - 2\nu_{\rho}\nu_z = -\psi_z\psi_{\rho}, \quad (6)$$

along with the Klein-Gordon equation

$$\psi_{zz} + \psi_{\rho\rho} + \rho^{-1}\psi_{\rho} = 0. \quad (7)$$

It is easy to see that if  $\nu_o$  and  $\zeta_o$  solve the vacuum Einstein equations, a solution to equations (3-7) is then given by

$$\nu = \nu_o + C \log \rho, \quad (8)$$

$$\zeta = B \zeta_o + E \nu_o + F \log \rho, \quad (9)$$

$$\psi = A \nu_o + D \log \rho, \quad (10)$$

where the constants are subject to the following constraints:

$$2C + AD = E, \quad (11)$$

$$A^2 + 2 = 2B, \quad (12)$$

$$D^2 + 2C^2 = 2F. \quad (13)$$

For the purposes of this work we will discard the logarithmic terms by setting the constants  $C, F$  and  $D$  to zero, ensuring thus asymptotic flatness at spatial infinity in a static case.

Once the solution with a massless scalar field metric has been constructed, we transform it into a non-static solution with a self-interacting scalar field with an exponential potential. This is accomplished by using an algorithm originally due to Fonarev (1995); see as well the generalization by Feinstein, Ibáñez & Lazkoz (1995). The new solution in a synchronous system of coordinates reads

$$ds^2 = -e^{2\nu(\rho,z)} dt^2 + R^2(t) e^{-2\nu(\rho,z)} \left( \rho^2 d\phi^2 + e^{2\zeta(\rho,z)} (d\rho^2 + dz^2) \right), \quad (14)$$

where the “scale factor” is  $R(t) = t^{2/k^2}$  and the new metric functions are

$$\nu = \nu_o \quad \text{and} \quad \zeta = (1 + 2/k^2) \zeta_o, \quad (15)$$

the constant  $k$  being the slope of the potential  $V = \Lambda e^{-k\psi}$  and  $\Lambda = (12 - 2k^2)/k^4$ . The line element in equation (14) is a solution of the Einstein field equations with the energy momentum tensor given by

$$T_{ab} = \psi_{,a}\psi_{,b} - g_{ab} \left( \frac{1}{2}\psi_{,i}\psi^{,i} + \Lambda e^{-k\psi} \right). \quad (16)$$

Furthermore, the new scalar field  $\psi(t, \rho, z)$  splits into a homogeneous and an inhomogeneous part,  $\psi(t, \rho, z) = \psi_h + \psi_{inh}$  with  $\psi_h$  and  $\psi_{inh}$  given by

$$\psi_h = \frac{2}{k} \log t \quad \text{and} \quad \psi_{inh} = \frac{2}{k} \nu_o. \quad (17)$$

Note that in the particular case  $k^2 = 6$  the potential term vanishes, and one is left with a massless scalar field.

## 2.2. Interpretation of the new solutions

As long as the seed static metric is asymptotically flat, the newly generated non-static solution is asymptotically homogeneous and isotropic, and at spatial infinity the geometry is represented by the FRW metric

$$ds^2 = -dt^2 + t^{4/k^2} (\rho^2 d\phi^2 + d\rho^2 + dz^2). \quad (18)$$

We now identify the homogeneous part of the scalar field with the velocity potential of an irrotational perfect fluid which is the source of the metric in equation (18). The energy-momentum tensor is then

$$T_{ab}^{FRW} = (p + \mu)u_a u_b + p g_{ab}, \quad (19)$$

where the four-velocity of the fluid is given by

$$u_a = \frac{\psi_{h,a} \delta_t^a}{\sqrt{(-\psi_{h,t} \psi^{h,t})}}, \quad (20)$$

so that the pressure  $p$  and the energy density  $\mu$  become

$$\mu = -\frac{1}{2} \psi_{h,t} \psi^{h,t} + \Lambda t^{-2} \quad \text{and} \quad p = -\frac{1}{2} \psi_{h,t} \psi^{h,t} - \Lambda t^{-2}. \quad (21)$$

Substituting the expression for the scalar field we readily get

$$p = \frac{4k^2 - 12}{t^2 k^4} \quad \text{and} \quad \mu = \frac{12}{t^2 k^4}. \quad (22)$$

It is straightforward to see that equation (22) defines the barotropic equation of state

$$p = \gamma \mu \quad \text{and} \quad \gamma = \frac{k^2 - 3}{3}. \quad (23)$$

Note, however, that the scalar field has also an inhomogeneous component. Although the inhomogeneities steadily dilute as the spatial distance increases, they cannot be regarded to be negligible in the intermediate regions.

It is well-known that as long as the gradient of the scalar field is timelike the energy momentum tensor can be interpreted in terms of a perfect fluid. The asymptotic homogeneity of the solution ensures that at any time the gradient of the scalar field is timelike outside a certain closed spatial region, depending basically on the mass and compactness of the disk, as well as on the strength of the scalar field. Outside this region the perfect fluid interpretation holds, and at spatial infinity the fluid becomes homogeneous and isotropic as mentioned above.

On the other hand, the evolution of the local inhomogeneities with time may also be deduced by studying the gradient of the scalar field:

$$\psi_{,c}\psi^{,c} = \psi_{h,c}\psi^{h,c} + \psi_{inh,c}\psi^{inh,c}, \quad (24)$$

where

$$\psi_{h,c}\psi^{h,c} = -\frac{4}{3\gamma+3}t^{-2}e^{-2\nu}, \quad (25)$$

and

$$\psi_{inh,c}\psi^{inh,c} = \frac{4}{3\gamma+3}t^{-\frac{4}{3\gamma+3}}e^{2\nu-2\zeta}(\nu_{,\rho}^2 + \nu_{,z}^2). \quad (26)$$

We have checked numerically that for the models with accelerated expansion  $\gamma < -1/3$  the outer region, where the homogeneous term of the scalar field dominates the one representing the spatial gradients, grows with time. On the other hand, the highly irregular inner region shrinks to zero. This behaviour is similar to that one found in the inflationary scenario, in the sense that the small-scale inhomogeneities are washed away due to the accelerated expansion.

The highly inhomogeneous region surrounding the disk plane where the perfect fluid interpretation is not valid may be thought of as playing the role of a cushion between the disk and the cosmological fluid, representing a transition region between both regimes.

We suggest, therefore, to interpret the solutions of the type given by equation (14) as describing an inhomogeneity embedded in an expanding Universe on the grounds that on large scales one recovers the Friedmannian behaviour while the local structure for small distances is governed by the seed metric. This interpretation will be re-enforced in the light of the results of following sections.

### 3. Relativistic expanding thin disks

We now apply the described algorithm to the well-known family of axially symmetric solutions representing infinitesimally thin disks in a relativistic context and construct their dynamical counterparts. We are mostly interested in the influence of the expansion on the kinematical quantities that characterize the disks. It is expected that for an expanding Universe the mass-energy density on the disk plane will steadily decrease as time goes by. However, the effect on other quantities such as velocity or angular momentum is not intuitively foreseeable. In addition, we believe that the conclusions reached in this work can bring a new perspective onto the problem of embedding irregular sources into standard cosmologies.

#### 3.1. Generation of thin disk families

The disk configurations we are dealing with were firstly studied by Morgan & Morgan (1969a, 1969b, 1970) and describe counterrotating disks with the same number of leftwise and rightwise rotating particles. As was pointed out in the previous section one can start with the Newtonian potential produced by a thin disk to obtain its relativistic version.

For the sake of simplicity, unless otherwise stated, we will focus the analysis on two families of disks, the Kuzmin-Curzon disks and the generalized Schwarzschild disks (BLK, 1993). The Kuzmin-Curzon disks may be used as building blocks for infinite families of more complicated disk-like solutions; one should just

superpose elementary Kuzmin-Curzon disks with different compacticities weighted by a function  $W(b)$ , as shown by Evans & de Zeeuw (1992). Their work on Newtonian axisymmetric potential-density pairs was extended to a relativistic case by BLK, who gave the general form of the metric for a superposition of Kuzmin-Curzon disks.

BLP gave a step further in the study of relativistic disks by constructing the more involved families of relativistic versions of the Kuzmin-Toomre (Toomre 1963; Nagai & Miyamoto 1976; Evans & de Zeeuw 1992) and Kalnajs-Mestel disks (Mestel 1963; Kalnajs 1976). The latter family of solutions is particularly interesting because they have long and flat rotation curves for certain values of the parameters, and include the so-called generalized Schwarzschild disks as their lowest order representatives.

The potential corresponding to a Kuzmin-Curzon disk is obtained by introducing a discontinuity in the original Curzon metric (Curzon 1924; Chazy 1924) using the transformation  $z \rightarrow |z| + b$ . This way of introducing the discontinuity is equivalent to placing two mirror particles of mass  $M$  at a distance  $b$  below and above the  $z = 0$  plane on the  $z$  axis. The Newtonian potential for the Kuzmin-Curzon disk is

$$\nu_o^{K-C} = -\frac{M}{[\rho^2 + (|z| + b)^2]^{\frac{1}{2}}}, \quad (27)$$

and following Weyl (1917), one identifies it with the metric function  $\nu_o$  in equation (10). This metric function remains a solution of the Laplace equation outside the  $z = 0$  plane, but now due to the discontinuity, there appears to be a non-vanishing surface mass density. Integration of the remaining metric function yields

$$\zeta_o^{K-C} = -\frac{M^2 \rho^2}{[\rho^2 + (|z| + b)^2]^2}. \quad (28)$$

Correspondingly, as shown by BLK, the classical surface mass density  $\Sigma(\rho) = 2\nu_{o,z}|_{z=0^+}^{z=0^-}$  is

$$\Sigma^{K-C} = \frac{4 M b}{(\rho^2 + b^2)^{\frac{3}{2}}}. \quad (29)$$

Here  $M$  is the total mass of the disk as measured from the infinity, and  $b$  is a parameter measuring the compactness of the disk.

The analogue of a generalized Schwarzschild disk is constructed in the classical Kuzmin's picture by substituting the two mirror particles by two rods with constant line density. Then, the general relativistic solution is given by

$$\nu_o^{G-S} = \frac{M}{b_{max} - b_{min}} \log \left| \frac{\rho_{min} + |z| + b_{min}}{\rho_{max} + |z| + b_{max}} \right|, \quad (30)$$

and

$$\zeta_o^{G-S} = \frac{2 M^2}{(b_{max} - b_{min})^2} \log \left| \frac{(\rho_{min} + \rho_{max})^2 - (b_{max} - b_{min})^2}{4 \rho_{min} \rho_{max}} \right|. \quad (31)$$

In this case, the classical surface mass density  $\Sigma(\rho)$  is

$$\Sigma^{G-S} = \frac{4 M}{(b_{max} - b_{min}) (\rho^2 + b^2)^{\frac{1}{2}}} \Bigg|_{b_{max}}^{b_{min}}, \quad (32)$$

where  $\rho_{min}^2 = \rho^2 + (|z| + b_{min})^2$  and  $\rho_{max}^2 = \rho^2 + (|z| + b_{min})^2$ ,  $b_{max} - b_{min}$  being the parameter that measures the compactness of the disk.

### 3.2. Disks in an expanding FRW Universe

We start by looking somewhat more carefully at the stress-energy tensor for the solutions given by equation (14) with the metric functions corresponding to a generic thin counterrotating disk.

In order to deal with the discontinuities in the metric across the  $z = 0$  plane, we consider the metric functions in the sense of distributions and introduce a new variable  $\xi = |z|$ . Generically, the metric coefficients will have square-integrable weak derivatives, and so the usual formula for the Ricci tensor can be interpreted in the sense of distributions. The stress-energy tensor reads (cf. as well Chamorro, Gregory & Stewart, 1987):

$$T_\rho^\rho - T_z^z = 2 R(t)^{-2} (\rho^{-1} \zeta_{,\rho} + \nu_{,\xi}^2 - \nu_{,\rho}^2) e^{-2\zeta+2\nu}, \quad (33)$$

$$T_\rho^\rho + T_z^z = -2 R(t)^{-2} (\dot{R}^2 + 2R\ddot{R}) e^{-2\nu}, \quad (34)$$

$$\begin{aligned} T_t^t + T_\phi^\phi &= -2 R(t)^{-2} (\nu_{,\rho\rho} + \nu_{,\xi\xi} + 2\delta(z)\nu_{,\xi} + \rho^{-1}\nu_{,\rho} - \zeta_{,\rho\rho} - \zeta_{,\xi\xi} \\ &\quad - 2\delta(z)\zeta_{,\xi} - \nu_{,\rho}^2 - \nu_{,\xi}^2) e^{-2\zeta+2\nu} \\ &\quad - 2 R(t)^{-2} (2\dot{R}^2 + R\ddot{R}) e^{-2\nu}, \end{aligned} \quad (35)$$

$$\begin{aligned} T_t^t - T_\phi^\phi &= -2 R(t)^{-2} (\nu_{,\rho\rho} + \nu_{,\xi\xi} + 2\delta(z)\nu_{,\xi} + \rho^{-1}\nu_{,\rho}) e^{-2\zeta+2\nu} \\ &\quad - 2 R(t)^{-2} (\dot{R}^2 - R\ddot{R}) e^{-2\nu}, \end{aligned} \quad (36)$$

$$T_z^z = -2 R(t)^{-2} [\theta(z) - \theta(-z)] (2\nu_{,\rho}\nu_{,\xi} - \rho^{-1}\zeta_{,\xi}) e^{-2\zeta+2\nu}, \quad (37)$$

$$T_t^t = 2 R(t)^{-3} \dot{R} \nu_{,\rho} e^{-2\zeta+2\nu}, \quad (38)$$

$$T_t^z = 2 R(t)^{-3} [\theta(z) - \theta(-z)] \dot{R} \nu_{,\xi} e^{-2\zeta+2\nu}. \quad (39)$$

The energy-momentum tensor given by equations (33-39) splits into a regular and a singular part proportional to the functional  $\delta(z)$ , which is interpreted as a thin counterrotating disk. We still separate the regular part into two bits: a highly inhomogeneous part vanishing at infinity that we interpret as an interaction term between the matter composing the disk and the cosmic fluid, and another part representing at infinity an isotropic perfect fluid. Phenomenologically we write

$$T_a^b = T_a^{b\,disk} + T_a^{b\,int} + e^{-2\nu} T_a^{b\,FRW}, \quad (40)$$

where

$$T_t^{t\,FRW} = 3 R(t)^{-2} \dot{R}^2, \quad (41)$$

and

$$T_\phi^{\phi\,FRW} = T_\rho^{\rho\,FRW} = T_z^{z\,FRW} = -2 R(t)^{-2} (\dot{R}^2 + 2R\ddot{R}). \quad (42)$$

The identification of the other terms is straightforward. The term we have referred to as  $T_a^{b\,disk}$  is precisely the one which is discontinuous across the  $z = 0$  plane and which therefore gives rise to the non vanishing mass density. One has to be careful when interpreting equation (40), for it has a purely phenomenological character. Obviously none of the three terms in the r.h.s. of equation (40) can be regarded as a true energy-momentum tensor, since they do not satisfy the energy conservation equation  $T_{;b}^{ab} = 0$  separately. Note, that this decomposition into three terms is similar to that proposed in §2.2 based on the character of the gradient of the scalar field. Both approaches qualitatively lead to the same physical description.

#### 4. Dynamics of expanding disks

In this Section we study the kinematical quantities of relativistic disks and discuss the influence of the expansion. We explicitly prove that the mass-energy density decreases with time, and also address the question of the effect of the expansion on the flattening of the rotation curves. Special attention will be paid to the comparison between a static disk and its counterpart in a pressure-free Universe. Our motivation is that the Universe, as observed at present, has negligible pressure.

We now look at the surface mass density and streaming velocities of the particles on the disk. The  $\tau_a^b$  surface components are obtained by integration across the disk of the  $T_a^b$  components of the energy-momentum tensor,

$$\tau_a^b = \int T_a^b R(t) e^{(\zeta-\nu)} dz. \quad (43)$$

As shown by BLK, the surface rest mass density in a fixed reference system reads  $\sigma_0 = 2\sigma_p(1-v^2)^{-1/2}$ , while the surface mass density in the same reference system is  $\sigma = 2\sigma_p(1-v^2)^{-1} = \sigma_0(1-v^2)^{-1/2}$ , where  $v$  is the rotational velocity and  $\sigma_p$  is the proper rest mass density of one stream.

We first calculate the surface mass density  $\sigma(\rho, t)$  on the disk plane by integrating the  $T_t^t$  term across the disk. Using equations (35,36) one gets

$$\sigma(\rho, t) = -\tau_t^t = - \int_{0-}^{0+} T_t^t R(t) e^{(\zeta-\nu)} dz = R(t)^{-1} e^{(\nu-\zeta)} (4\nu_{,\xi} - 2\zeta_{,\xi})|_{\xi=0}. \quad (44)$$

Substituting  $\zeta_{,\xi}$  as calculated from equation (6) we obtain after some algebra

$$\sigma(\rho, t) = 4 R(t)^{-1} \nu_{,\xi} e^{(\nu-\zeta)} (1 - \rho f(\gamma) \nu_{,\rho})|_{\xi=0}, \quad (45)$$

where we denote  $f(\gamma) = (3\gamma + 3)/(3\gamma + 5)$  and  $\gamma$  is the adiabatic index of the perfect fluid. Note that the static case will be recovered in the limit  $\gamma \rightarrow \infty$ ,  $f(\gamma) \rightarrow 1$ . The particular case of a dust filled Universe corresponds to  $\gamma = 0$  and  $f(\gamma) = 3/5$ .

By integrating the  $T_\phi^\phi$  term obtained from equations (35,36) one gets

$$v^2 \sigma = \tau_\phi^\phi = \int_{0-}^{0+} T_\phi^\phi R(t) e^{(\zeta-\nu)} dz = 2 R(t)^{-1} e^{(\nu-\zeta)} f(\gamma) \zeta_{,\xi}|_{\xi=0}, \quad (46)$$

or alternatively

$$v^2 \sigma = 4 R(t)^{-1} e^{(\nu-\zeta)} \rho f(\gamma) \nu_{,\rho} \nu_{,\xi}|_{\xi=0}. \quad (47)$$

Then, from equations (45,47) one readily obtains the expression for the square of the streaming velocities

$$v^2 = \frac{\rho f(\gamma) \nu_{,\rho}}{1 - \rho f(\gamma) \nu_{,\rho}} \Big|_{\xi=0}. \quad (48)$$

In order to emphasize the difference in the flattening of the rotation curves in the static and expanding cases we also evaluate the derivative of the velocity in the radial direction obtaining

$$v_{,\rho} = - \frac{f(\gamma)^{1/2} \nu_{,\xi\xi}}{2 [\nu_{,\rho} (1 - \rho f(\gamma) \nu_{,\rho})]^{1/2}} \Big|_{\xi=0}. \quad (49)$$



Since the classical mass density  $\Sigma(r) = 4\nu_{,\xi}|_{\xi=0}$  of the disks is positive everywhere, in order to ensure the positivity of the surface energy density  $\sigma$  we must impose  $\rho f(\gamma)\nu_{,\rho}|_{\xi=0} < 1$ , as deduced from equation (45). This is equivalent to the fulfillment of the weak energy condition (cf. BLK). For the particular case of an expanding Kuzmin-Curzon disk this restriction reduces to

$$\frac{M f(\gamma)}{b} < \frac{\sqrt{27}}{2}, \quad (50)$$

whereas for a generalized Schwarzschild disk it becomes

$$\frac{M f(\gamma)}{(b_{max} - b_{min})} < \frac{[1 - (b_{min}/b_{max})^2]^{\frac{1}{2}}}{[1 - (b_{min}/b_{max})^{\frac{2}{3}}]^{\frac{3}{2}}}, \quad (51)$$

therefore, the expanding disks may be denser than their static counterparts.

Moreover, if  $\rho f(\gamma)\nu_{,\rho}|_{\xi=0} < 1/2$  the dominant energy-condition holds and the rotation velocities are subluminal. It is clear that as long as the dominant energy condition holds the positivity of the mass density is also ensured.

To compare the streaming velocities of a static disk and any of its time-evolving counterparts, one may look at the expression of their quotient, which reads

$$\frac{v^2(\gamma)}{v^2(\gamma = \infty)} = f(\gamma) \frac{1 - \rho\nu_{,\rho}}{1 - \rho f(\gamma)\nu_{,\rho}} \Big|_{\xi=0}. \quad (52)$$

Since  $f(\gamma) \leq 1$ , we conclude that for expanding disks the velocities are typically everywhere lower than those for a static one (see Figure 1).

To compare our results with those obtained by BLK we represent the kinematical quantities as functions of the *circumferential* radius  $\rho_c = \rho e^{-\nu}$ , where  $2\pi\rho_c$  is the physical circumference of a circle with radius  $\rho = \text{constant}$ . Note that for the solutions studied in this paper the comoving radius does not depend on the adiabatic index  $\gamma$ .

Yet, more interesting conclusions are obtained from the quotient between the velocity derivatives in the radial direction,

$$\frac{v_{,\rho}(\gamma)}{v_{,\rho}(\gamma = \infty)} = f^{1/2}(\gamma) \left( \frac{1 - \rho\nu_{,\rho}}{1 - \rho f(\gamma)\nu_{,\rho}} \right)^{3/2} \Big|_{\xi=0}. \quad (53)$$

From equation (53) it can be learnt that the slope of the rotation curves for expanding disks is less pronounced than for static ones. It can be concluded that the expansion accentuates the flattening of the rotation curves (see Figure 2).

Another question to dwell on is the effect of the expansion on the mass-energy density on the disk plane. Similarly, as done above with the velocities and their radial derivatives, we look at the quotient of the mass energy density of an evolving and a static disk:

$$\frac{\sigma(\gamma)}{\sigma(\gamma = \infty)} = \frac{1 - \rho f(\gamma)\nu_{,\rho}}{1 - \rho\nu_{,\rho}} (t e^{\zeta_0})^{-\frac{2}{3\gamma+3}}. \quad (54)$$

Since  $\zeta_0$  is negative everywhere on the disk, we conclude that expanding disks are denser than static ones, with additional mass concentrated outside the center, whereas the central density is not affected by the expansion. Time-evolution of this quantity crucially depends on the adiabatic index  $\gamma$ . To be more specific,

the mass-density dilution rate increases, keeps constant or decreases with time, if the expansion parameter  $\gamma$  is smaller, equal or larger than  $-1/3$  respectively.

It is also interesting to examine the surface rest mass density of the rotating particles as measured in a frame attached to fixed axes. This quantity is given by

$$\sigma_0 = \sigma (1 - v^2)^{1/2}. \quad (55)$$

Substituting the expression for  $\sigma$  and  $v$  in equations (45,48) we get

$$\sigma_0(\rho, t) = 4\nu_{,\xi} e^{(\nu-\zeta)} [1 - \rho f(\gamma) \nu_{,\rho}]^{\frac{1}{2}} [1 - 2\rho f(\gamma) \nu_{,\rho}]^{\frac{1}{2}} \Big|_{\xi=0}. \quad (56)$$

The latter quantity is everywhere positive provided the dominant energy condition holds. Taking the previous results into account it is straightforward to see that the influence of the expansion on the surface rest mass density  $\sigma_0$  is the same as for the mass density  $\sigma$ .

We have further defined a new function  $\Delta\sigma/\sigma \equiv [\sigma(\gamma) - \sigma(\gamma = \infty)]/\sigma(\gamma)$  which gives the contrast in surface mass density between an expanding and a static disk. Figures 3a and 3b represent the contrast function  $\Delta\sigma/\sigma$  and Figures 4a and 4b give their rest counterparts  $\Delta\sigma_0/\sigma_0$  for both a generalized Schwarzschild disk and a Kuzmin-Curzon disk. It can be learnt from the figures that the expanding disks with the same mass parameter  $M$  are much denser than their static counterparts.

Finally, it is worth looking at the specific angular momentum of the counterrotating components of the disk. Bearing in mind that the specific angular momentum of a particle with rest mass  $m$  rotating at radius  $r$  is defined as

$$j = (p_\phi \phi / m) = g_{\phi\phi} d\phi / d\lambda, \quad (57)$$

where  $\lambda$  is proper time, then

$$j(\rho, t) = R(t) \frac{\rho v e^{-\nu}}{(1 - v^2)^{\frac{1}{2}}} \Big|_{\xi=0}, \quad (58)$$

or alternatively

$$j(\rho, t) = R(t) \frac{(\rho^3 f(\gamma) \nu_{,\rho})^{\frac{1}{2}} e^{-\nu}}{(1 - 2\rho f(\gamma) \nu_{,\rho})^{\frac{1}{2}}} \Big|_{\xi=0}. \quad (59)$$

Similarly to what happened with the rotation velocities, a smaller  $\gamma$  gives a smaller angular momentum, which increases with time. This behaviour is presented in Figures 5a and 5b where we compare the specific angular momentum in an expanding and a static case for a generalized Schwarzschild disk and a Kuzmin-Curzon disk.

## 5. Conclusions and outlook

We have constructed exact solutions to Einstein equations which we interpret as representing relativistic disks in a cosmological setting. A self interacting scalar field serves as a source of the global expansion, yet locally it defines a disk-like structure across the  $z = 0$  plane. Far away from this plane the gradient of the scalar field may be identified with the velocity potential of an irrotational perfect fluid with an adiabatic equation of state  $p = \gamma\rho$ . Near the azimuthal plane the spatial gradients of the scalar field dominate over the kinetic part and the geometry is highly inhomogeneous. No sharp-cut transition region exists in between these two different regimes, however, this probably corresponds to a physically more realistic situation than

a surface matching between different solutions of gravitational field equations. Moreover, to the best of our knowledge, there do not exist such solutions in the case of axial symmetry and an external FRW geometry.

Some particular cases of the solutions we have obtained ( $k^2 = 6$ ) may be re-interpreted as disks in the Brans-Dicke theory. Indeed, in this case the scalar field may be considered as massless (the potential term vanishes) and a simple conformal transformation  $ds^2 \rightarrow e^{\psi/\sqrt{\omega+3/2}} ds^2$  transforms the solution into a Brans-Dicke frame (Tabensky and Taub 1973). The physical interpretation of the solutions then is quite different: these represent relativistic disks in a theory where the gravitational constant varies in space and time. We will not dwell more about this point here, but just mention that the analysis of our paper applies equally well to Brans-Dicke disks.

Once the solutions are interpreted as local inhomogeneities in a model Universe the way is cleared to see the effects produced by expansion. We have found that depending on the rate of expansion the inhomogeneities occupy larger or smaller regions of the Universe. More specifically, for the accelerated expansion we find that inhomogeneities disappear with time, while in a decelerated model their growth is unbounded.

The effect of the expansion on the kinematical characteristics of the disks was studied as well. We have shown that expansion changes in principle the fall-off of the rotational curves, the angular momentum and the surface mass density of the disks. We have also compared the characteristics of the static disks with those in a dust filled Universe.

Although we have concentrated our study on disk-like objects, it is remarkable that the generating technique used to obtain solutions is also adequate to study other type of sources of astrophysical interest such as cosmic strings, walls, spherical shells, etc.

## 6. Acknowledgements

We are grateful to Wyn Evans, Sasha Kashlinsky, Konrad Kuijken and M. A. Vázquez-Mozo for correspondence and valuable suggestions. This work was partially supported by a Spanish Ministry of Education Grant (CICYT) PB93-0507 and a Basque Country University Grant UPV/EHU/72.310EBO36/95. R.L. acknowledges financial support from the Basque Government under Fellowship BFI94-094.

## REFERENCES

- Bertola, F., Cinzano, P., Corsini, E.M., Pizzella, A., Persic, M., & Salucci, P. 1996, *ApJ*, 458, L67
- Bičák, J., Ledvinka, T. 1993, *Phys. Rev. Lett.* 71, 1669
- Bičák, J., Lynden-Bell, D., & Katz, J. 1993, *Phys. Rev. D* 47, 4334
- Bičák, J., Lynden-Bell, D., & Pichon, C. 1993, *MNRAS*, 265, 126
- Curzon, H. E. J. 1924, *Proc. London Math. Soc.* 23, 477
- Chamorro, A., Gregory, R., & Stewart, J. M. 1987, *Proc. R. Soc. London A*, 413, 251
- Chazy, J. 1924, *Bull. Soc. Math. Paris* 52, 17

- Evans, N. W., & de Zeeuw, P. T. 1992, MNRAS, 257, 152
- Feinstein, A., Ibáñez, J., & Lazkoz, R. 1995, Class. Quantum. Grav., 12, L57
- Fonarev, O. A. 1995, Class. Quantum. Grav., 12, 1739
- Kalnajs, A., 1976, ApJ, 205, 751
- Kuijken, K., Fisher D., & Merrifield, M. R.. 1996, MNRAS, 283, 543
- Kuzmin, G. G. 1956, Astron. Zh., 33, 27
- Lemos, J. P. S., & Ventura, O. S. 1994, J. Math. Phys., 35, 3604
- Lemos J. P. S., & Letelier, P. S. 1993, Class. Quantum Grav., 10, L75
- Lemos J. P. S., & Letelier, P. S. 1994, Phys. Rev. D, 49, 5135
- Lemos J. P. S., & Letelier, P. S. 1996, Int. J. Mod. Phys. D, 5, 53
- Levi-Civita, T. 1919a, Rend. Acad. Lincei, 28, 3
- Levi-Civita, T. 1919b, Rend. Acad. Lincei, 28, 101
- Noerslinger, P.D., & Petrosian, V. 1971, 168, 1
- Lynden-Bell, D., & and Pichon, C. 1996, MNRAS, 280, 1007
- Merrifield, M.R., & Kuijken, K. 1994, ApJ, 432, 575
- Mestel L. 1963, MNRAS, 126, 553
- Morgan, T., & Morgan, L. 1969a, Phys. Rev., 183, 1097
- Morgan, T., & Morgan, L. 1969b, Phys. Rev., 188, 2544 (E)
- Morgan, T., & Morgan, L. 1970, Phys. Rev. D, 2, 2576
- Nagai, R., & Miyamoto, M. 1976, PASJ, 28, 1
- Rix, H., Fisher, H., & Illingworth, D. 1992, ApJ, 400, L5
- Tabensky, R., & Taub, A.H. 1973, Commun. Math. Phys. 29, 61
- Toomre, A., 1963, ApJ, 138, 385
- Weyl, H. 1917, Ann. Phys. (N.Y.), 54, 307

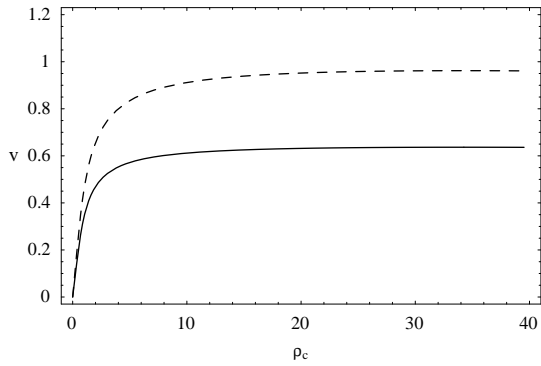


Fig. 1a

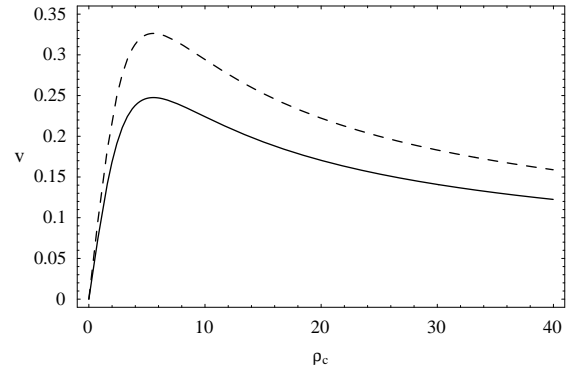


Fig. 1b

Fig. 1.— Streaming velocity  $v$  as function of the circumferential radius  $\rho_c$  for a generalized Schwarzschild disk with  $M = 100$ ,  $b_{min} = 1$  and  $b_{max} = 200$  (a); and for a Kuzmin-Curzon disk with  $M = 1$  and  $b = 4$  (b). The continuous lines correspond to expanding disks in a dust filled FRW Universe, whereas the dashed lines correspond to their static counterparts.

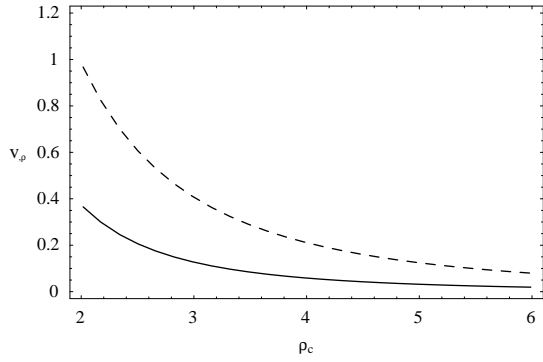


Fig. 2a

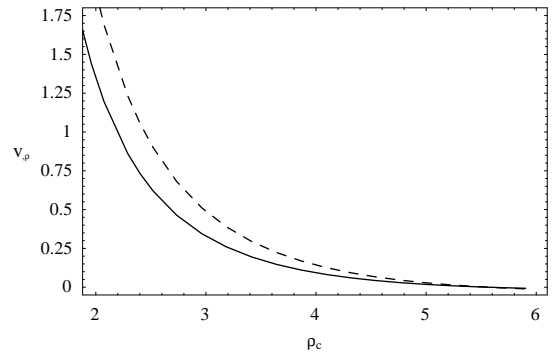


Fig. 2b

Fig. 2.— Radial derivative of the streaming velocity  $v_\rho$  as function of the circumferential radius  $\rho_c$  for a generalized Schwarzschild disk with  $M = 100$ ,  $b_{min} = 1$  and  $b_{max} = 200$  (a); and a Kuzmin-Curzon disk with  $M = 1$  and  $b = 4$  (b). The continuous lines corresponds to expanding disks in a dust filled FRW Universe, whereas the dashed lines correspond to their static counterparts.

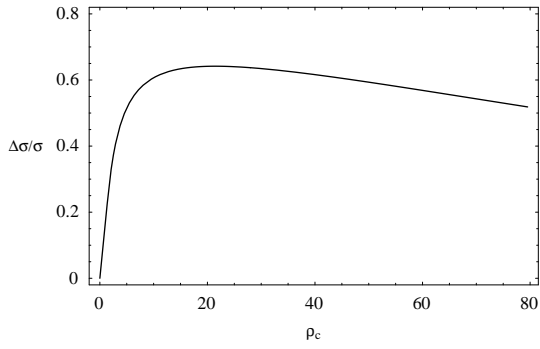


Fig. 3a

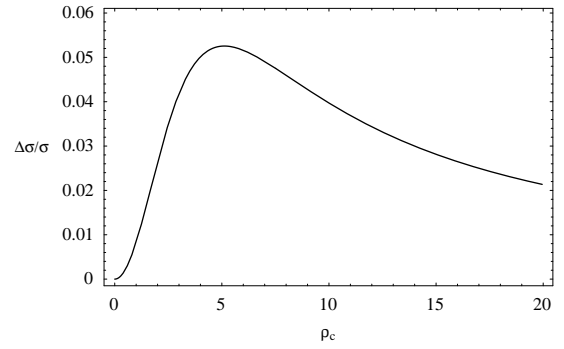


Fig. 3b

Fig. 3.— Surface energy density contrast  $\Delta\sigma/\sigma$  at  $t = 1$  as function of the circumferential radius  $\rho_c$  for a generalized Schwarzschild disk with  $M = 100$ ,  $b_{min} = 1$  and  $b_{max} = 200$  (a); and for Kuzmin-Curzon disk with  $M = 1$  and  $b = 4$  (b).

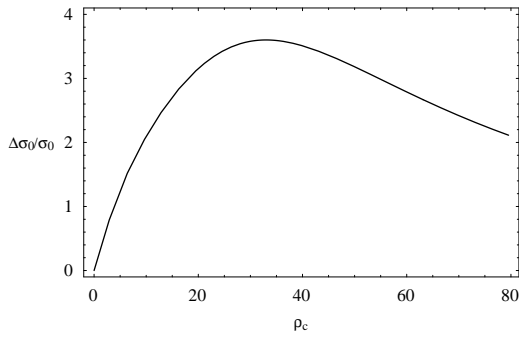


Fig. 4a

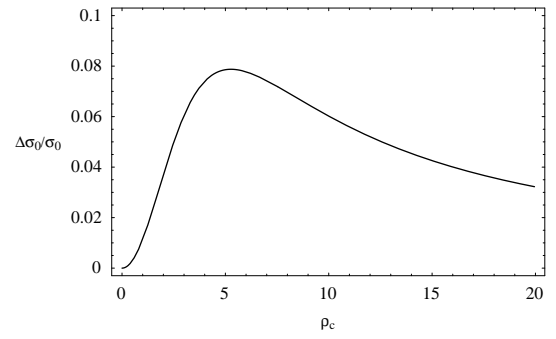


Fig. 4b

Fig. 4.— Surface rest energy density contrast  $\Delta\sigma_0/\sigma_0$  at  $t = 1$  as function of the circumferential radius  $\rho_c$  for a generalized Schwarzschild disk with  $M = 100$ ,  $b_{min} = 1$  and  $b_{max} = 200$  (a); and a Kuzmin-Curzon disk with  $M = 1$  and  $b = 4$  (b).



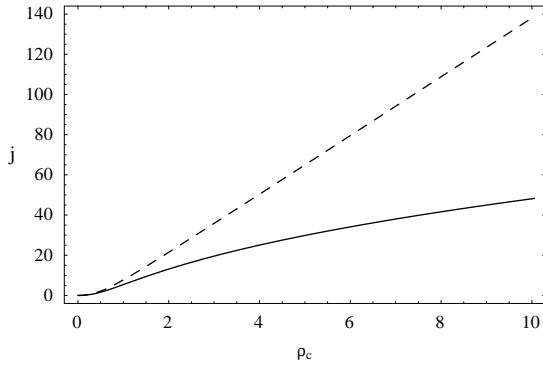


Fig. 5a

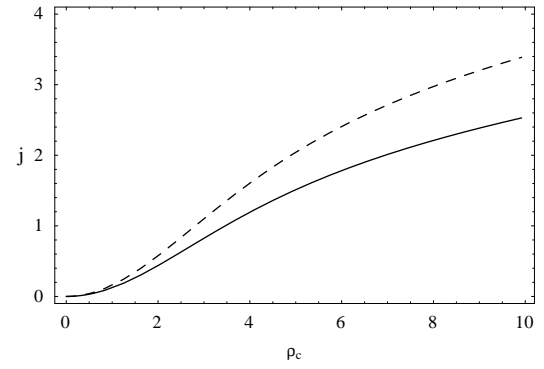


Fig. 5b

Fig. 5.— Specific angular momentum  $j$  at  $t = 1$  as function of the circumferential radius  $\rho_c$  for a generalized Schwarzschild disk with  $M = 100$ ,  $b_{min} = 1$  and  $b_{max} = 200$  (a); and for a Kuzmin-Curzon disk with  $M = 1$  and  $b = 4$  (b). The continuous lines correspond to disks in a dust filled FRW Universe, whereas the dashed lines correspond to their static counterparts.